NJC

Accepted Manuscript

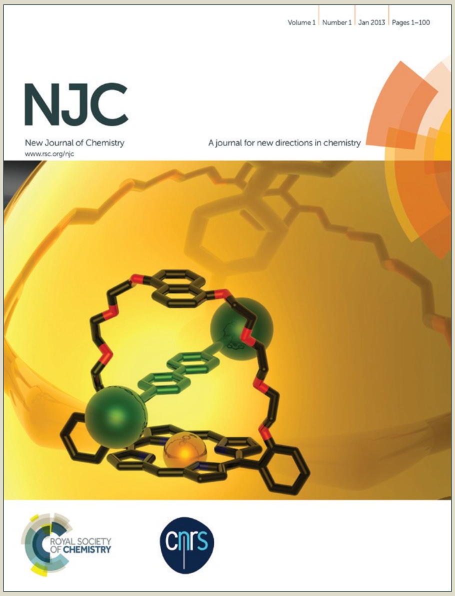

Volume 1 | Number 1 | Jan 2013 | Pages 1–100

NJC

New Journal of Chemistry
www.rsc.org/njc

A journal for new directions in chemistry

ROYAL SOCIETY OF CHEMISTRY

ROYAL SOCIETY OF CHEMISTRY

www.rsc.org/njc

Journal Name RSCPublishing

ARTICLE

Synthesis and Characterization of $CsSrCO_3F$ – A Beryllium-Free New Deep-Ultraviolet Nonlinear Optical Material

Qingfei Li,[a,b] Guohong Zou,*[b] Chensheng Lin[c] and Ning Ye*[c]

Cite this: DOI: 10.1039/x0xx00000x

Received 00th January 2015,
Accepted 00th January 2015

DOI: 10.1039/x0xx00000x

www.rsc.org/

A new noncentrosymmetric (NCS) material, namely, $CsSrCO_3F$ was synthesized through conventional solid state reactions. $CsSrCO_3F$ exhibits a 3-dimensional structure that is composed of the stacked layers of $[Sr(CO_3)]_\infty$, and the coplanar alignment of $[CO_3]$ triangles. Each $[Sr(CO_3)]_\infty$ layer is connected by infinite Sr–F–Sr chains. Powder second-harmonic generation (SHG) using the Kurtz−Perry technique shows that $CsSrCO_3F$ is type I phase-matchable, and the measured SHG coefficient was 1.2 times that of KH_2PO_4. The result from the UV-vis diffuse reflectance spectroscopy study of the powder samples indicated that the short-wavelength absorption edge was below 200 nm, suggesting that $CsSrCO_3F$ is a promising deep-UV nonlinear optical material.

Introduction

Deep-UV nonlinear optical (NLO) crystals[1] which can generate deep-UV coherent light (λ <200nm) have become increasingly important and are attracting more attention owing to its promising applications in photolithography, micro-machining, advanced instrument development, laser cooling and attosecond pulse generation. In spite of many reports in the literature,[2] it is an ongoing challenge to obtain practically useful materials possessing high NLO coefficients and wide UV transparency, especially those covering the deep-UV region. In the past decades, many efforts have been made to search for new deep-UV nonlinear optical crystals. Non-centrosymmetric (NCS) borates[3] are the most common materials for deep-UV NLO applications such as β-BaB_2O_4 (BBO),[3b] LiB_3O_5 (LBO),[3c] CsB_3O_5 (CBO)[3f] and $CsLiB_6O_{10}$ (CLBO),[3g,3h] $SrBe_2BO_7$ (SBBO),[3e] and $K_2Al_2B_2O_7$ (KABO).[3i] And recently a new series of beryllium borates[4] have been synthesized which has already been proved to be promising deep-UV nonlinear optical materials. But so far only $KBe_2BO_3F_2$ (KBBF)[3d] is capable of generating coherent light below 200nm using direct SHG methods for example: 6th harmonic generation of 1064nm (Nd:YAG) radiation to 177.3nm. However, KBBF has a very strong layer habit with respect to crystal growth which hinders its practical applications. Also, the synthesis and crystal growth of KBBF need to use highly toxic BeO which complicates the detailed investigation of their properties. Thus, it presents great interest to search for deep-UV NLO materials that do not contain beryllium.

Mixed-metal carbonate fluorides[5] have been proved to be a promising materials family for deep-UV NLO applications in our previous research.[5a] We introduced alkaline fluoride into alkaline earth carbonates and synthesized a family of fluoride carbonates such as $KCaCO_3F$,[5a] $KSrCO_3F$,[5a] $RbCaCO_3F$,[5a] $RbSrCO_3F$.[5a] All of them exhibit two unique attributes, there is no dangling oxygen atom in $(CO_3)^{2-}$ units and the inclusion of fluoride blue-shifts the absorption edge, which guarantee the materials are much more amenable to transmission in the deep-UV region. Ye's group also discovered a few more NCS mixed metal fluoride carbonates such as $Na_8Lu_2(CO_3)_6F_2$,[5b] $Na_3Lu(CO_3)_2F_2$,[5b] $KCdCO_3F$,[5c, 5d] $RbCdCO_3F$,[5c, 5d] $KZnCO_3F$[5c] $RbZnCO_3F$[5c] and $CsPbCO_3F$.[5e] Halasyamani's group recently synthesized $K_{2.70}Pb_{5.15}(CO_3)_5F_3$[6a] and $RbPbCO_3F$[6b] along with a new deep-UV NLO material, $RbMgCO_3F$.[6c]

As we known, fluoride carbonates with the formula $A^+M^{2+}CO_3F$ (A represents alkali metal elements, M represents divalent metal elements) are good candidate materials for deep-UV NLO applications. The crystal structures of $A^+M^{2+}CO_3F$-type compounds exhibit the stacking of $[AF]_\infty$and $[M(CO_3)]_\infty$ layers, and the coplanar alignment of $[CO_3]$ triangles. The ratio of ionic radii between A^+ and M^{2+} are strongly correlated with the arrangement of $[CO_3]$ groups which can be divided into four groups:[5c] (i) 1.21 to 1.34 for isostructures of $KSrCO_3F$, $RbSrCO_3F$ and $KCaCO_3F$; (ii) 1.53 to 1.66 for the two isostructures of $RbCaCO_3F$ and $CsCaCO_3F$; (iii) 1.67 to 2.16 for $ATCO_3F$ (A=K, Rb; T=Zn, Cd); (iv) 2.29 for $RbMgCO_3F$. In order to ensure high transmission in the deep-UV region, alkali and alkaline earth metals should be chosen as the counter cations in mixed metal fluoride carbonates because there are no d–d electron or f–f electron transitions in this spectral region. We calculated the ratio of ionic radii between Cs^+ and Sr^{2+} which is 1.57 belonging to group (ii) (1.53-1.66) and our investigation of the Cs-Sr-CO_3-F system resulted in the discovery of a new deep-UV NLO fluoride carbonate material, namely $CsSrCO_3F$. Herein we report the syntheses, crystal structures, optical properties, thermal stability and NLO properties.

Experimental section

Synthesis

Polycrystalline samples of $CsSrCO_3F$ were synthesized through standard solid-state reactions. Stoichiometric amounts of Cs_2CO_3 (Alfa Aesar, 99%), SrF_2 (Alfa Aesar, 99%) and $SrCO_3$ (Alfa Aesar, 99%) were thoroughly mixed with agate mortars and pestles and pressed into pellets. The pellets were heated at 550 °C for 120 h, and cooled down to room temperature rapidly at a rate of 10 °C/min with several intermediate grinding steps in between each heating. Single crystal growing trials of $CsSrCO_3F$ with different fluxes have not been successful; SrF_2 crystals were obtained for most runs.

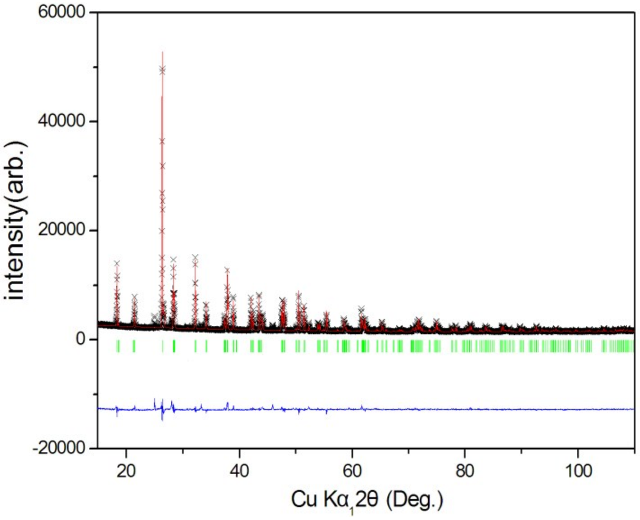

Fig. 1 Experimental, calculated, and difference X-ray diffraction plots for $CsSrCO_3F$. The calculated pattern (red solid line) is compared with the observed data (×). The locations of the reflections are indicated by the green vertical bars. The difference between the observed and calculated profiles is shown at the bottom (blue solid line).

Powder X-ray diffraction (PXRD)

The PXRD data were collected on a Bruker D8-Advance diffractometer using Cu Ka radiation at room temperature with 40 kV and 40 mA. The 2θ range was 5–110° with a step size of 0.02°, and a step time of 1 s. The structure of the reported material was refined using the Rietveld method with the GSAS program.[7] The refinements of the products were carried out in the NCS space group, *P*-62*m* (No. 189) with a starting model of the reported single-crystal data of $CsCaCO_3F$.[5a] The experimental, calculated, and difference diffraction plots for $CsSrCO_3F$ are shown in Fig. 1. The crystallographic data and refinement results of $CsSrCO_3F$ are summarized in Table 1. Atomic coordinates and isotropic displacement parameters of the reported materials can be found in the ESI.

Table1 Summary of crystallographic data and refinement results of $CsSrCO_3F$

Formula	$CsSrCO_3F$
fw	230.51
Space group	*P*-62*m*
$a = b$/Å	9.6286(2)
c/Å	4.7482(2)
V/Å^3	381.23(11)
Z	3
$R_p{}^a$	0.0514
$R_{wp}{}^b$	0.0921

$^aR_p = \Sigma |I_o - I_c| / \Sigma I_o$. $^bR_{wp} = [\Sigma w |I_o - I_c|^2 / \Sigma w I_o^2]^{1/2}$.

Thermal analysis

The TG/DTA scans were measured on a NETZSCH STA 449C simultaneous analyzer. Reference (Al_2O_3) and polycrystalline samples (5-15 mg) were enclosed in Al_2O_3 crucibles and heated from room temperature to 900 °C at a rate of 10 °C/min under a constant flow of nitrogen gas.

Infrared (IR) spectroscopy

Infrared spectra of the samples were recorded on a Thermo Scientific Nicolet 6700 FT-IR spectrometer in the 400–4000 cm^{-1} ranges, with the samples embedded in KBr matrices.

UV-vis diffuse reflectance spectroscopy

UV-vis diffuse reflectance spectra were obtained on a Varian Cary 500 scan UV-vis-NIR spectrophotometer over the spectral range 200–2500 nm at room temperature. The reflectance spectra were transformed into absorbance using the Kubelka–Munk function.[8]

Second-harmonic generation (SHG) measurements

Powder second-harmonic generation (SHG) signals were measured using the experimental method adapted from that reported by Kurtz and Perry[9] with the wavelength of the fundamental (1064 nm doubled to 532 nm). Since SHG efficiencies were known to be strongly dependent on particle size, polycrystalline samples were ground and sieved into the following particle size ranges: 20-44, 44-74, 74-105, 105-149, and 149-210 μm. In order to make relevant comparisons with known SHG materials, crystalline KDP were also ground and sieved into the same particle size ranges. The samples were pressed between glass microscope cover slides and secured with tape in 1-mm thick aluminum holders containing an 8-mm diameter hole. They were subsequently placed in a light-tight box and irradiated with a pulsed infrared beam (10 ns, 3 mJ, 10 Hz) from a Q-switched Nd: YAG laser at a wavelength of 1064 nm. A cutoff filter was used to limit background flash-lamp light on the sample, and an interference filter (530 ± 10 nm) was used to select the second harmonic for detection with a photomultiplier tube attached to a RIGOL DS1052E 50-MHz oscilloscope. This procedure was then repeated using the standard nonlinear optical material KDP, and the ratio of the second-harmonic intensity outputs was calculated. No index-matching fluid was used in any of the experiments.

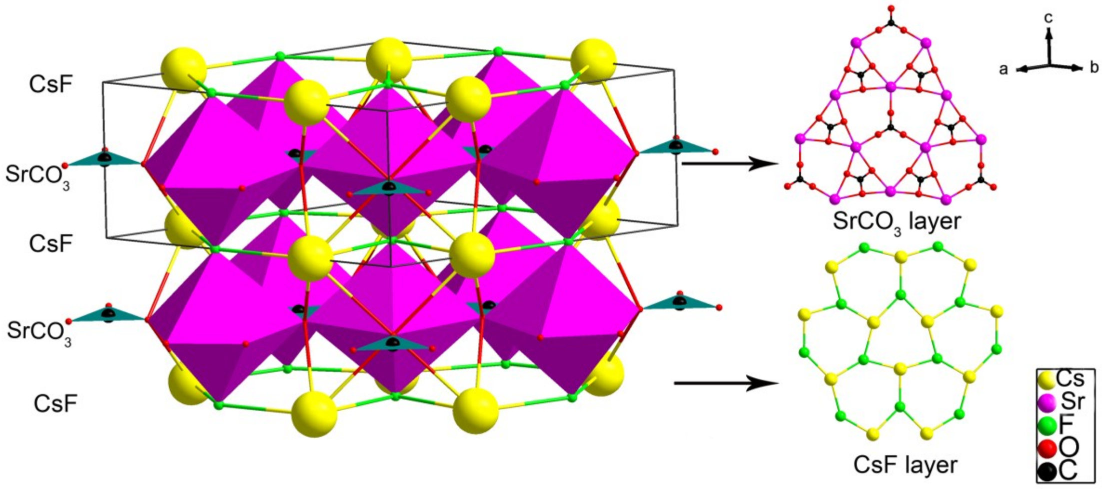

Fig. 2 Crystal structure of $CsSrCO_3F$.

Computational details

First principle band structure and density of states (DOS) calculations were carried out by employing the plane-wave basis pseudopotential method as implemented in the CASTEP.[10] The exchange and correlation effects were considered by Perdew−Burke−Ernzerhof (PBE) in the generalized gradient approximation (GGA).[11] Norm-conserving pseudopotentialsare selected to describe the interactions between the ionic cores and the valence electrons.[12] In the atoms, C $2s^22p^2$, O $2s^22p4$, F $2s^22p^5$, Cs $5s^25p^66s^1$ and Sr $4s^24p^65s^2$ were treated as valence electrons. A kinetic-energy cutoff of 700 eV was set for the self-consistent-field convergence of the total electronic energy. Monkhorst–Pack *k*-point meshes with a density of 4 × 4 × 7 points in the Brillouin zone of the $CsSrCO_3F$ unit cell are chosen. The other parameters and convergence criteria were adopted the default values of the CASTEP code.

Results and discussion

Crystal structure description

$CsSrCO_3F$ crystallizes in a hexagonal crystal system with an acentric space group of *P*-62*m* (No. 189). As shown in Figure 2, The structure is made up of alternately stacked layers of $[Sr(CO_3)]_\infty$ and $[CsF]_\infty$, and all the adjacent layers are connected by infinite Sr–F–Sr chains parallel to the c-axis, forming a three-dimensional network. The C atoms are coordinated to three O atoms to form planar $[CO_3]$ triangles with C-O bond lengths ranging from 1.2882 to 1.3153 Å and O-C-O bond angles at 120.00 (3)°. The Cs atom is found to coordinate to eight oxygen and three fluorine atoms. And the Sr atom is 7-fold coordinated forming a $[SrO_5F_2]$ pentagonal bipyramid which is connected to three CO_3 groups by sharing its five equatorial oxygen atoms (two edge-sharing and one corner-sharing). Within a single $SrCO_3$ layer, one third of the three CO_3 groups is aligned antiparallel to the other two, making only one third of contribution to the SHG coefficients.

A series of $A^+M^{2+}CO_3F$-type compounds have been synthesized. All of them exhibit the stacking of $[AF]_\infty$and $[M(CO_3)]_\infty$layers, and the coplanar alignment of $[CO_3]$ triangles. on the basis of the ratio of ionic radii between A^+ and M^{2+} which are strongly correlated with the arrangement of $[CO_3]$ groups, they can be divided into four groups: (i) 1.21 to 1.34 for isostructures of $KSrCO_3F$, $RbSrCO_3F$ and $KCaCO_3F$ in which the M atom is 8-fold coordinated forming a $[MO_6F_2]$ hexagonal bipyramid sharing edges with three CO_3 groups; (ii) 1.53 to 1.66 for the three isostructures of $RbCaCO_3F$, $CsCaCO_3F$ and $CsSrCO_3F$, in which the M atom is 7-fold coordinated forming a $[MO_5F_2]$ pentagonal bipyramid sharing corners with one and edges with two CO_3 groups; (iii) 1.67 to 2.16 for $ATCO_3F$ (A=K, Rb; T=Zn, Cd) in which the M atom is 5-fold coordinated forming a $[MO_3F_2]$ trigonal bipyramid sharing corners with three CO_3 groups; (iv) 2.29 for $RbMgCO_3F$ in which the M atom is 6-fold coordinated forming a $[MO_4F_2]$ quadrilateral bipyramid sharing corners with two and edges with one CO_3 groups.

The bond valence sums for $CsSrCO_3F$ are calculated using the formula,

$$V_i = \sum_j S_{ij} = \sum_j \exp\left\{\left(r_0 - r_{ij}\right)/B\right\}$$

where S_{ij} is the bond valence associated with the bond lengths r_{ij} and r_0, and B is an empirically determined parameter (usually 0.37).[13] The calculated total bond valence for Cs, Sr, C, O and F atoms are summarized in Table S1 in the Supporting Information. These results indicate that the Cs, Sr, C, O and F atoms in $CsSrCO_3F$ are in the +1, +2, +4, -2 and -1 oxidation states, respectively.

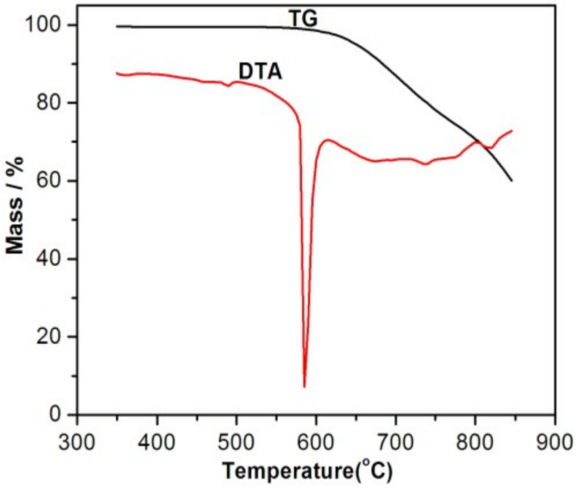

Fig. 3 TGA/DTA diagrams of $CsSrCO_3F$.

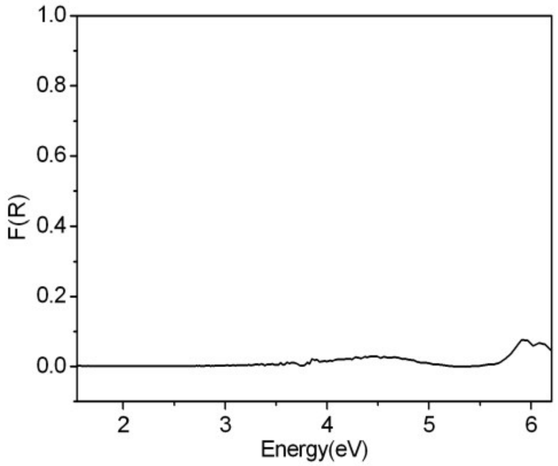

Fig. 4 UV-vis absorption spectra and optical diffuse reflectance spectra of $CsSrCO_3F$.

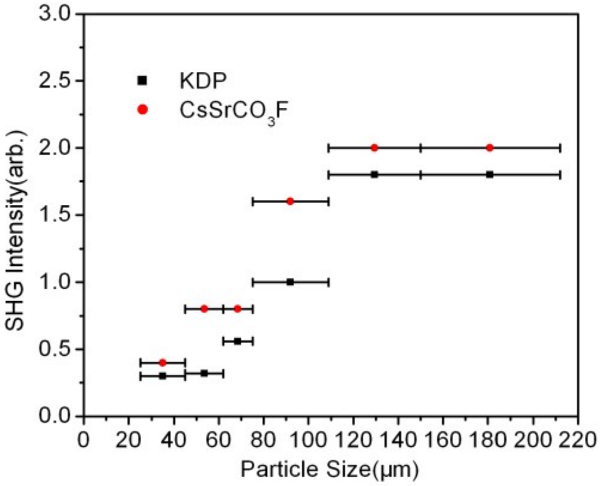

Fig. 5 SHG measurements of $CsSrCO_3F$.

Thermal properties

As shown in Figure 3, the DTA curve of $CsSrCO_3F$ shows one endothermic peak along with weight loss on the TGA curves at its melting points. Analysis of the powder XRD pattern of the residues (Figure S1) revealed that $CsSrCO_3F$ was decomposed into SrF_2, SrO and Cs_2O, suggesting that it is incongruently melting compound in the air. The decomposition reaction is $2CsSrCO_3F \rightarrow SrF_2 + SrO + Cs_2O + 2CO_2$ (g).

Optical Properties

Figure S2 presents the IR spectra of $CsSrCO_3F$ which revealed C–O vibrations between 1500–650 cm^{-1}. The strong broad bands observed at 1421 cm^{-1} and small bands at 1031 cm^{-1} can be assigned to the stretching C–O vibrations. The out-of-plane vibration, δ(OCO), is observed at 841 cm^{-1} as a medium band, and the peak at 708 cm^{-1} is attributed to bending vibration δ(OCO). The small bands at 1810 cm^{-1} can be assigned to the stretching C=O vibrations.

The UV-vis diffuse reflectance spectra were collected for $CsSrCO_3F$ (see Fig. 4). Absorption (*K*/*S*) data were calculated from the following Kubelka-Munk function:

$$F(R) = \frac{(1-R)^2}{2R} = \frac{K}{S}$$

where *R* is the reflectance, *K* is the absorption, and *S* is the scattering.[8] In the (*K*/*S*)-versus-*E* plots, extrapolating the linear part of the rising curve to zero provides the onset of absorption. No obvious absorption peak in the range of 6.22 — 1.55eV (corresponding to 200 — 800 nm) was observed, indicating that $CsSrCO_3F$ may be potentially applied in deep-UV NLO materials.

Nonlinear optical (NLO) properties

The curves of SHG signal as a function of particle size from the measurements made on ground polycrystalline $CsSrCO_3F$ are shown in Fig. 5. The results are consistent with phase-matching behaviors according to the rule proposed by Kurtz and Perry.[9] KDP was used as the reference. The second-harmonic signal is found to be 1.2 times as large as d_{36} (KDP) which is 0.39 pm/V.[14]

According to the anionic group theory,[15] the dipole transition from the cations to the anionic groups is the off-site transition. Its value is about one order smaller than the dipole transition of the intra-atomic transitions within anionic groups. So the contribution to the SHG coefficients of $CsSrCO_3F$ from the anionic groups $[CO_3]^{2-}$ is dominant, which is much larger than that of the charge transfer between the s-states of cations and the p-originated states of anions. Therefore the macroscopic second-order susceptibility $\chi^{(2)}$ could be expressed by Eq.(1) on the basis of the anionic group theory,

$$\chi_{ijk}^{(2)} = \frac{F}{V}\sum_{P}\sum_{i'j'k'}\alpha_{ii'}\alpha_{jj'}\alpha_{kk'}\beta_{i'j'k'}^{(2)}(P) \quad P=[CO_3]^{2-} \qquad (1)$$

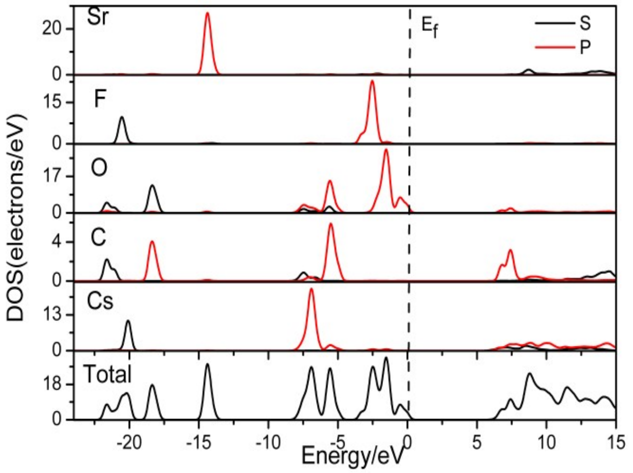

Fig. 6 Total and partial densities of states for $CsSrCO_3F$.

where F is the correction factor of the localized field; V is the volume of the unit cell; $\alpha_{ii'}$, $\alpha_{jj'}$, and $\alpha_{kk'}$ are the direction cosines between the macroscopic coordinates of the crystal and the microscopic coordinates of $[CO_3]^{2-}$ groups, and $\beta^{(2)}_{i'j'k'}$ is the microscopic second-order susceptibility tensors of an individual group. Owing to the fact that $[CO_3]^{2-}$ is a planar group in point group D_{3h}, there are only two nonvanishing second-order susceptibility $\beta^{(2)}_{111}=\beta^{(2)}_{222}$ due to the point group operation. Because the geometrical factor, g, can be derived from eq. (2), eq.(1) may be simplified:

$$x^{(2)}_{\mathrm{ijk}} = \frac{F}{V} \cdot \mathrm{g}_{\mathrm{ijk}} \cdot \beta^{(2)}_{111}$$

$$\mathrm{g}_{ijk} = \sum_{P}^{n} [\alpha(\mathrm{i}1)\alpha(j1)\alpha(k1) - \alpha(\mathrm{i}1)\alpha(j2)\alpha(k2) - \alpha(\mathrm{i}2)\alpha(j1)\alpha(k2) - \alpha(\mathrm{i}2)\alpha(j2)\alpha(k1)]$$

$$g = \max(\mathrm{g}_{ijk}); (\mathrm{i}, \mathrm{j}, \mathrm{k} = 1,2,3) \qquad (2)$$

In case of unspontaneous polarization, the structural criterion C is defined as:

$$C = \frac{g}{n} \qquad (3)$$

so Eq.(2) may be simplified according to the deduction process shown in the reference 16

$$\chi^{(2)}_{\mathrm{ijk}} = \mathrm{F} \times (\mathrm{n/V}) \times \mathrm{C} \times \beta_{111}([\mathrm{CO}_3]) \qquad (4)$$

Where n is the number of anionic groups in a unit cell. So the NLO coefficient $\chi^{(2)}_{ijk}$ is proportional to density of the $[CO_3]^{2-}$ group (n/V) and the structural criterion (C). To gain further insight the SHG effects as determined by the arrangement of the NLO-active groups and the density of NLO-active groups, the coefficient of NLO effect for $CsSrCO_3F$ was calculated and compared with the synthesized fluoride carbonates NLO materials (Table 2). In the crystal structures of $KSrCO_3F$, $RbSrCO_3F$ and $KCaCO_3F$, the $[CO_3]$ triangles are all exactly parallel to each other, giving a 100% optimum. For $CsSrCO_3F$, as its isostructural compounds $RbCaCO_3F$ and $CsCaCO_3F$, one third of the $[CO_3]$ triangles are anti-parallel to the others and results in a C value of 33.33% which leads to a moderate SHG coefficient. As shown in table 2, the above argument on the structure-properties correlations is in good agreement with the SHG measurement.

Table 2 NLO effects of $AMCO_3F$ (A=K, Rb, Cs; M=Ca, Sr)

Crystals	SHG coefficient (×KDP)	structual criterion C	Densities of $[CO_3]$ (n/V) (Å^{-3})	(n/V)×C (Å^{-3})
$KCaCO_3F$	3.61	1.00	0.00998	0.00998
$KSrCO_3F$	3.33	1.00	0.00889	0.00889
$RbSrCO_3F$	3.33	1.00	0.00858	0.00858
$RbCaCO_3F$	1.11	0.33	0.00921	0.00304
$CsCaCO_3F$	1.11	0.33	0.00882	0.00291
$CsSrCO_3F$	1.2	0.33	0.00787	0.00263

Theoretical Calculations

The band structures are presented in the SI Figure S3. Compound $CsSrCO_3F$ exhibits an indirect band gap of 5.984 eV. The calculated value is smaller than the experimental value because of the common underestimation of the band gap by the DFT method. The total and partial densities of states (DOS and PDOS) for $CsSrCO_3F$ are presented in Figure 6. The valence band in the range from -22.5 to -17.5 eV comes from mostly O-2s2p and C-2s2p with a small amount of Cs-6s and F-2s states. The peak localized around -14.0 eV almost arises from Sr-4p. The bands near the Fermi level (from -10.0 to 0 eV in the valence band and from 6.0 to 8.1 eV in the conduction band) are mainly predominately derived from the O-2s2p, C-2s2p, F-2p and Cs-5p. Thus, the electron transition is mainly contributed by inside excitation of the $[CO_3]^{2-}$ group. Because of the above analysis, the NLO effect of $CsSrCO_3F$ mainly stems from the $[CO_3]^{2-}$ groups, and the anti-parallel spatial arrangement and relatively high density of $[CO_3]^{2-}$ led to a moderate NLO effect.

Conclusions

A new noncentrosymmetric fluoride carbonate, namely, $CsSrCO_3F$ was synthesized through conventional solid state reactions. In the crystal structure, alternately stacked layers of $[Sr(CO_3)]_\infty$ and $[CsF]_\infty$ are connected by infinite Sr–F–Sr chains parallel to the c-axis to form a three-dimensional network. Within a single $SrCO_3$ layer, one third of the three CO_3 groups align antiparallel to the other two, making only one third of contribution to the SHG coefficients to get a moderate SHG coefficients about 1.2 times as large as that of d_{36}(KDP). Powder second-harmonic generation using the Kurtz−Perry technique shows that $CsSrCO_3F$ is type I phase-matchable. The result from the UV-vis diffuse reflectance spectroscopy study of the powder samples indicated that the short-wavelength absorption edge was below 200 nm, suggesting that $CsSrCO_3F$ is a promising deep-UV nonlinear optical material.

Acknowledgements

This research was supported by the National Natural Science Foundation of China (Nos.21401178, 21501161 and 91222204).

Notes and references

[a] *Institute of Atomic and Molecular Physics, Sichuan University, Chengdu, 610065, P. R. China.*
[b] *Institute of Chemical Materials and Advanced Materials Research Center, Key Laboratory of Science and Technology on High Energy Laser, China Academy of Engineering Physics, Mianyang, 621900, P. R. China. E-mail: zough@caep.cn;*
[c] *Fujian Institute of Research on the Structure of Matter, Key Laboratory of Optoelectronic Materials Chemistry and Physics, Chinese Academy of Sciences, Fuzhou, 350002, P. R. China. E-mail: nye@fjirsm.ac.cn*

†Electronic Supplementary Information (ESI) available: Atomic coordinates and isotropic displacement parameters, selected bond distances and angles, infrared spectra, PXRD patterns of thermal decomposition products, and band structures for $CsSrCO_3F$.
See DOI: 10.1039/b000000x/

1. (a) P. S. Halasyamani and K. R. Poeppelmeier, *Chem. Mater.*, 1998, **10**, 2753; (b) H. S. Ra, K. M. Ok and P. S. Halasyamani, *J. Am. Chem. Soc.*, 2003, **125**, 7764; (c) R. E. Sykora, K. M. Ok, P. S. Halasyamani and T. E. Albrecht-Schmitt, *J. Am. Chem. Soc.*, 2002, **124**, 1951; (d) H. Ye, D. Fu, Y. Zhang, W. Zhang, R. G. Xiong and S. D. Huang, *J. Am. Chem. Soc.*, 2009, **131**, 42; (e) Y. Z. Huang, L. M. Wu, X. T. Wu, L. H. Li, L. Chen and Y. F. Zhang, *J. Am. Chem. Soc.*, 2010, **132**, 12788.
2. (a) F. Kong, S. P. Huang, Z. M. Sun, J.-G. Mao and W. D. Cheng, *J. Am. Chem. Soc*., 2006, **128**, 7750; (b) H. Y. Chang, S. H. Kim, P. S. Halasyamani and K. M. Ok, *J. Am. Chem. Soc.*, 2009, **131**, 2426; (c) C. F. Sun, C. L. Hu, X. Xu, J. B. Ling, T. Hu, F. Kong, X. F. Long and J.-G. Mao, *J. Am. Chem. Soc.*, 2009, **131**, 9486; (d) E. O. Chi, K. M. Ok, Y. Porter and P. S. Halasyamani, *Chem. Mater.*, 2006, **18**, 2070; (e) S. L. Pan, J. P. Smit, B. Watkins, M. R. Marvel, C. L. Stern and K. R. Poeppelmeier, *J. Am. Chem. Soc.*, 2006, **128**, 11631; (f) S.-w. Bae, C.-Y. Kim, D. W. Lee and Ok, K. M., *Inorg. Chem.*, 2014, **53**, 11328; (g) G. Zou, Z. Ma, K. Wu and N. Ye, *J. Mater. Chem.*, 2012, **22**, 19911; (h) L. Huang, G. Zou, H. Cai, S. Wang, C. Lin and N. Ye, *J. Mater. Chem. C*, 2015, **3**, 5268.
3. (a) P. Becker, *Adv. Mater.*, 1998, **10**, 979; (b) C. T. Chen, B. C. Wu, A. D. Jiang and G. M. You, *Sci. Sin. B-Chem. Biol. Agr. Med. Earth Sci.*, 1985, **28**, 235; (c) C. T. Chen, Y. C . Wu, A. D. Jiang, B. C. Wu, G. M. You, R. K. Li and S. J. Lin, *J. Opt. Soc. Am. B-Opt. Phys*, 1989, **6**, 616; (d) L. Mei, Y. Wang, C. Chen and B. Wu, *J. Appl. Phys*., 1993**, 74**, 7014; (e) C. T. Chen, Y. B. Wang, B. C. Wu, K. C. Wu, W. L. Zeng and L. H. Yu, *Nature,* 1995, **373**, 322; (f) Y. C . Wu, T. Sasaki, S. Nakai, A. Yokotani, H. G. Tang and C. T. Chen, Appl. Phys. Lett., 1993, **62**, 2614; (g) Y. Mori, I. Kuroda, S. Nakajima, T. Sasaki and S. Nakai, Appl. Phys. Lett., 1995, **67**, 1818; (h) J. M. Tu and D. A. Keszler, Mater. Res. Bull., 1995, **30**, 209; (i) Z. G. Hu, T. Higashiyama, M. Yoshimura, Y. K. Yap, Y. Mori and T. Sasaki, Jpn. J. Appl. Phys., 1998 , **37**, 1093; (j) R. Komatsu. Appl. Phys. Lett., 1997, **70**, 3492. (k) H. Wu, S. Pan, K. R. Poeppelmeier, H. Li, D. Jia, Z. Chen, X. Fan, Y. Yang, J. M. Rondinelli and H. Luo, *J. Am. Chem. Soc.*, 2011, **133**, 7786; (l) Y. Shi, S. Pan, X. Dong, Y. Wang, M. Zhang, F. Zhang and Z. Zhou, *Inorg. Chem.*, 2012, **51**, 10870; (m) X. Xu, C. L. Hu, F. Kong, J. H. Zhang, J. G. Mao and J. Sun, *Inorg. Chem.*, 2013, **52**, 5831; (n) X. Fan, L. Zang, M. Zhang, H. Qiu, Z. Wang, J. Yin, H. Jia, S. Pan and C. Wang, *Chem. Mater.*, 2014, **26**, 3169; (o) J. L. Song, C. L. Hu, X. Xu, F. Kong and J. G. Mao, *Angew. Chem., Int. Ed.*, 2015, **54**, 3679; (p) H. P. Wu, S. L. Pan, K. R. Poeppelmeier, H. Y. Li, D. Z. Jia, Z. H. Chen, X. Y. Fan, Y. Yang, J. M. Rondinelli and H. S. Luo, *J. Am. Chem. So,* 2011, **133**, 7786; (q) H. W. Yu, S. L. Pan, H. P. Wu and Z. H. Yang, *J. Mater. Chem*. 2012, **22**, 2105; (r) H. W. Yu, H. P. Wu, S. L. Pan, Z. H. Yang and K. R. Poeppelmeier, *J. Am. Chem. Soc.,* 2014, **136**, 1264.
4. (a) S. C. Wang, N. Ye, W. Li and D. Zhao, *J. Am. Chem. Soc.,* 2010, **132**, 8779; (b) S. C. Wang and N. Ye, *J. Am. Chem. Soc.,* 2011, **133**, 11458.
5. (a) G. Zou, N. Ye, L. Huang and X. S. Lin, *J. Am. Chem. Soc.,* 2011, **133**, 20001; (b) M. Luo, G. Zou, N. Ye, C. S. Lin and W. D. Cheng, *Chem. Mater.*, 2013, **25**, 3147; (c) G. Yang, G. Peng, N. Ye, *Chem. Mater.* DOI: 10.1021/acs.chemmater.5b03890; (d) G. Zou, G. Nam, K. M. Ok, RSC Adv., 2015, 5, 84754; (e) G. Zou, L. Huang, N. Ye, C. S. Lin, W. D. Cheng and H. Huang, *J. Am. Chem. Soc.*, 2013, **135**, 18560.
6. (a) T. Tran and P. S. Halasyamani, *Inorg. Chem.*, 2013, **52**, 2466; (b) T. Tran, P. S. Halasyamani and J. M. Rondinelli, *Inorg. Chem.*, 2014, **53**, 6241; (c) T. Tran, J. G. He, J. M. Rondinelli and P. S. Halasyamani, *J. Am. Chem. Soc.*, 2015, **137**, 10504..
7. A. C. Larson and R. B. von Dreele, *General Structural Analysis System (GSAS)*, Los Alamos National Laboratory, Los Alamos, NM, 1987.
8. (a) P. Kubelka and F. *Z.* Munk, *Tech. Phys*, 1931, **12**, 593; (b) J. Tauc, *Mater. Res. Bull,* 1970, **5**, 721.
9. S. K. Kurtz and T. T. Perry, *J. Appl. Phys.*, 1968, **39**, 3798.
10. (a) J. H. Lin, L. P. You, G. X. Lu, L. Q.Yang, M. Z. Su, *J. Mater. Chem*, 1998, **8**, 1051; (b) W. W. Zhao, S. L. Pan, J. Han, Z. X. Zhou, X. L. Tian, J. J. Li, *Inorg. Chem. Commun*, 2011, **14**, 566.
11. (a) I. D. Brown, D. Altermatt, *Acta Crystallogr.* 1985*,* **B41**, 244; (b) N. E. Brese, M. O'Keeffe, *Acta Crystallogr.* 1991, **B47**, 192.
12. J. S. Lin, A. Qteish, M. C. Payne, V. Heine, Phys. Rev. B, 1993, **47**, 4174.
13. (a) I. D. Brown and D. Altermatt, *Acta Crystallogr*. 1985, **B41**, 244; (b) N. E. Brese and M. O'Keeffe, *Acta Crystallogr*. 1991, **B47**, 192.
14. R. C. Eckardt, H. Masuda, Y. X. Fan and R. L. Byer, *IEEE J. Quantum Electron. QE*, 1990, **26**, 922.
15. (a) C. T. Chen, *Sci. Sin. (Engl. Ed.)* 1979, **22**, 756; (b) C. T. Chen and G. Z. Liu, *Annu. Rev. Mater. Sci*., 1986, **16**, 203; (c) C. T. Chen, Y. C . Wu and R. K. Li, *Int. Rev. Phys. Chem.*, 1989, **8**, 65.
16. N. Ye, Q. X. Chen, B. C. Wu, C. T. Chen, *J. Appl. Phys.,* 1998, **84**, 555.

The table of contents entry

A noncentrosymmetric fluoride carbonate $CsSrCO_3F$ has been synthesized which is a promising beryllium-free deep-UV nonlinear optical material.